Finite Element Analysis of Different Hip Implant Designs along with Femur under Static Loading Conditions

Chethan K. N.[1], Shyamasunder Bhat N.[2], Zuber M.[3], Satish Shenoy B.[4]*

[1]MTech, Assistant Professor, Department of Aeronautical and Automobile Engineering, Manipal Institute of Technology, Manipal Academy of Higher Education, Manipal-576104, Karnataka, India
[2]MBBS, MS, DNB, Professor, Department of Orthopedics, Kasturba medical college, Manipal Academy of Higher Education, Manipal-576104, Karnataka, India
[3]PhD, Associate Professor, Department of Aeronautical and Automobile Engineering, Manipal Institute of Technology, Manipal Academy of Higher Education, Manipal-576104, Karnataka, India
[4]PhD, Professor, Department of Aeronautical and Automobile Engineering, Manipal Institute of Technology, Manipal Academy of Higher Education, Manipal-576104, Karnataka, India

ABSTRACT

Background: The hip joint is the largest joint after the knee, which gives stability to the whole human structure. The hip joint consists of a femoral head which articulates with the acetabulum. Due to age and wear between the joints, these joints need to be replaced with implants which can function just as a natural joint. Since the early 19th century, the hip joint arthroplasty has evolved, and many advances have been taken in the field which improved the whole procedure. Currently, there is a wide variety of implants available varying in the length of stem, shapes, and sizes.

Material and Methods: In this analytical study of femur, circular, oval, ellipse and trapezoidal-shaped stem designs are considered in the present study. The human femur is modeled using Mimics. CATIA V-6 is used to model the implant models. Static structural analysis is carried out using ANSYS R-19 to evaluate the best implant design.

Results: All the four hip implants exhibited the von Mises stresses, lesser than its yielded strength. However, circular and trapezoidal-shaped stems have less von Mises stress compared to ellipse and oval.

Conclusion: This study shows the behavior of different implant designs when their cross-sections are varied. Further, these implants can be considered for dynamic analysis considering different gait cycles. By optimizing the implant design, life expectancy of the implant can be improved, which will avoid the revision of the hip implant in active adult patients.

Citation: Chethan K. N, Shyamasunder Bhat N, Zuber M, Satish Shenoy B. Finite Element Analysis of Different Hip Implant Designs along with Femur under Static Loading Conditions. *J Biomed Phys Eng*. 2019;9(5):507-516. https://doi.org/10.31661/jbpe.v0i0.1210.

Keywords

Von mises stress; Hip Prosthesis; Finite element analysis; Static analysis; Total deformation; Femur

Introduction

At the time of birth, the human body consists of around 270 bones, and it will be reduced to 206 at the time of adulthood as some of the bones are fused together [1]. The hip joint transmits the load from the upper body to the lower abdomen [2]. The average length of hip bone will be 45cms in adult which is approximate ¼th of an adult height [3]. The hip joint is a synovial joint that fixes the lower limb to the trunk. It provides a wide range of movements which comprises a socket (acetabulum), and synovial ball (femoral head). With an increase in the femoral head size, the range of motions increases with an increase

*Corresponding author:
B .Satish Shenoy
Department of Aeronautical and Automobile Engineering, Manipal Institute of Technology, Manipal Academy of Higher Education, Manipal-576104, Karnataka, India
E-mail: satish.shenoy@manipal.edu

Received: 27 May 2019
Accepted: 19 August 2019

in the movement of the joint [4]. However, the size of the joint depends on the individual anatomy. Hip femoral head diametral sizes vary from 22mm to 54mm depending upon the person's anatomy and range of motions required. The hip joint can support the complete weight of the body while providing stability mainly during the movement of the trunk on the femur, as taking place during walking and running [5].

The femoral head is articulated into the pelvis and gives the joint different degrees of freedom, which helps the joint movement [6]. With the trauma or injuries and due to the age, these joints must be replaced by artificial implants. Early from 1935, the hip arthroplasty was a successful medical procedure which then was used for any type of hip joint disorders. Total hip arthroplasty is commonly known as one of the best advanced techniques in healthcare [7,8]. Sir Charnley was considered as the key designer for total hip joint arthroplasty. In total hip arthroplasty, the femoral head is separated from the acetabulum by introducing a bearing surface between the two parts. By this procedure, the pain is drastically reduced, and motion is restored. The stems are the primary components that give stability after the arthroplasty [9]. Over the stem, the femoral head is fitted by press fit, followed by an acetabular cup and backing cup. Presently, hip joint arthroplasty has a success rate of 10 years and 95% survivorship for the patients elder than seventy years [10,11]. Different biomaterials have been used as bearing surfaces since the beginning of the hip joint prosthesis. The bearing couple used by orthopedic surgeons can be metal-on-polyethylene (MoP) and ceramic-on-polyethylene (CoP), which are well-known as hard-on-soft bearings; and metal-on-metal (MoM), ceramic-on-ceramic (CoC) and ceramic-on-metal (CoM), which are well-known as hard-on-hard bearings. Hard-on-soft bearings have suffered a long-term failure due to polyethylene wear debris induced osteolysis [11]. Osteolysis is the result of biological and biomechanical connections between the wear debris produced by the total hip arthroplasty and the environment. This depends on the wear volumes, size, and shape of the wear debris produced. Small submicron polyethylene wear particles elicit more powerful biological activities than larger particles [12]. Even though there are many types of materials, combinations are used to develop the implant. There is a limited life span for the implant, and it requires resurfacing after that, so there is a wide scope to develop the new biomaterials and enhanced designs of the implants which will last long more than ten years. There is a need to develop a long-lasting prosthesis that can be used for high demand younger and more active patients like elite athletes and professional sportspersons [13]. Gradually, more patients undergo total hip arthroplasty due to an active lifestyle and also injuries [14], and they are usually expected to uphold an advanced level of activity even after hip arthroplasty. In addition, life expectancy increases, which has placed an increasing demand on these arthroplasties. For these reasons, even though this is a highly positive operation, the number of revision procedures is expected to rise near future. So, it is required to improve the combination of material, design and the surgical procedures which will help to develop the new implants that can last long more than ten years in order to avoid the hip resurfacing over the period after the hip arthroplasty. Previously, many studies have been carried out to understand the behavior of different implants under different loading conditions [15-18]. In the present study, four different stem shapes are designed: a uniform femoral head ball size of 28mm, an acetabular cup of 4mm and a metal backing cup of 2mm are used [19,20]. All the components are modeled using CATIA V-6. The femur bone is modeled from the computed tomography images of a healthy femur bone scanned data set. Mimics is used to extract the femur model from the CT images. The complete hip implant is evaluated

along with the femur bone. The finite element method is widely used to analyze the different biomedical implants [21]. The static structural analysis is performed on these models using ANSYS R-19 to know the best design among these four models which are widely used presently.

Material and Methods

In this analytical study of femur, the institutional ethical clearance was obtained from Kasturba Medical College, MAHE, Manipal. Anonymized healthy male CT scans were obtained from Kasturba Medical College, Manipal for the present study [Age of the patient was 36 years and length of the femur was 461mm (Weight 76kgs)] [22]. Philips Brilliance 64 channel CT scanner was used to obtain the CT DICOM images with slice thickness 0.625mm. The average length of the adult femur of the Asian population is between 42 to 48cm, so it is between the value femur [3]. Three-dimensional models of the femur are developed using Mimics (Materialize, Leuven, Belgium) software in Digital Imaging and Communications in Medicine (DICOM) format [23]. Initially, segmentation is carried out with the change in density and with editing the mask option, the model is filtered to obtain a new geometry consisting exclusively of separate cancellous and cortical bone [24,25]. Once the three-dimensional bone is extracted from the Mimics, using the 3-Matic, the smoothing and wrapping of the bone model are carried out. Further, the model is used in CATIA V-6 for smoothing and removing the irregularities in the model outer geometry. The modeled femur bone mimics the natural joint [22]. To implant the designed stem into the femur, the femur is bisected from the greater trochanter and the femoral head is removed [26]. The shape of the stem will greatly affect the functionality and longevity of the implant. Cross-section of the stem with varying geometry will directly affect the stress distribution in the implant along with the deformation. In the present study, four different cross-section designs (circular, oval, ellipse and trapezoidal) are considered. The cross-sections are varied along with the length of the stem from the distal end. The trunnion is considered as 12/14mm for the models which are modeled, where the femoral head is going to be fitted into the stem. All these stem designs were modeled in CATIA V-6. The four different stems with varying cross-sections are shown in Figure 1.

The length of stems from the proximal end to distal end is 180mm, and this length is constant for all the stem designs. The uniform femoral head size of 28mm along with an acetabular cup of 4mm and backing cup of 2mm is mod-

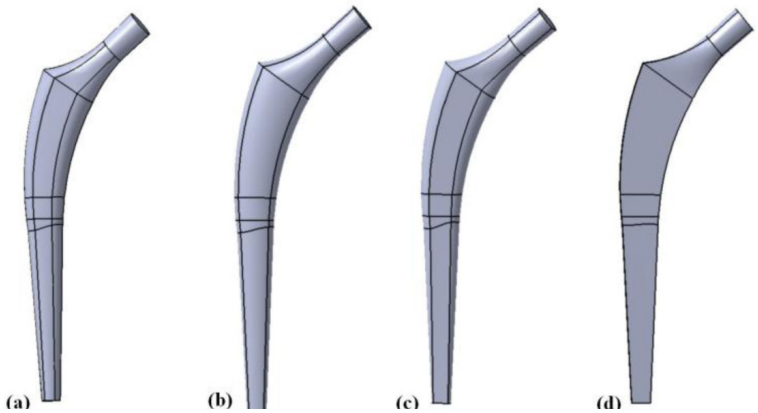

Figure 1: The different stem designs shapes (a) Circular, (b) Ellipse, (c) Oval, (d) Trapezoidal.

eled [27]. Using Boolean operation, all these components are joined together to replicate the complete hip prosthesis. The complete hip implant which is modeled with different cross-sections of stems, it is inserted into the femur bone. These implants are positioned into the bisected femur bone considering the patient's femur and pelvic anatomy [28]. These hip implants along with femur are used for the static structural analysis in ANSYS R-19 to evaluate the best implant design out of the developed four different models.

Boundary Conditions

To carry out the finite element analysis of non-modular femoral stems, the boundary conditions are applied as per the ASTM F299-13, and loading conditions are considered as per ISO 7206-4:2010(E) [29]. According to these standards, the modeled stems are bisected into three cross-sections, the first cut from the center of the head to 80mm. A second cut should be 10 mm below the first cut. The hip stem is constrained in all directions on all faces from the distal end to the second cut. Constraining the stem in this manner ensures that excessive erroneous stresses are not generated at the region of interest due to the influence of rigid fixation [29]. The femur bone is considered isotropic linear [30,31]. Ultra-high molecular weight polyethylene (UHMWPE), CoCrMo alloy, 316L stainless steel, and Ti-6Al-4V alloy are now used in the hip implants. In this study, stem, femoral head, and backing cup are considered as cobalt-chromium, and acetabular cup considered as ultra-high molecular polyethylene. This is the same as ceramic on polyethylene hip implant. The femur bone is extracted as separate cortical bone, cancellous bone and respective materials properties are assigned which will mimic natural human femur. The material properties considered for the study are given in Table 1.

Figure 2 shows the hip implant with applied boundary conditions and the complete discretized model.

Table 1: Mechanical properties of the different materials.

Sl no.	Materials	Young's modulus [GPa]	Density [gm/cm^3]	Poisson's ratio	Ultimate Tensile strength [MPa]	References
1.	Cortical bone	17	2	0.30	130	[32,33]
2.	Cancellous bone	0.52	1.08	0.29	-	[32,33]
3.	Co-Cr Alloy	200	8.5	0.30	1503	[32]
4.	UHMWPE	0.963	0.949	0.31	48	[34]

An unstructured mesh with a mesh size of 1mm is considered for the stem, acetabular cup, backing cup, and femoral head, and mesh size of 5mm is considered for the bone including cortical and cancellous bone. Output for mesh convergence study was the von Mises stress. With the previous study, the mesh convergence study was performed on the complete femur bone, and it was found that there is no change in the results with mesh size lesser than 5mm. So, femur mesh size is considered as 5mm to avoid the higher time for analysis [35]. These sizes are kept constant for all the four designs. Table 2 below shows the number of elements and nodes with respect to different stem designs.

Results

The femur bone consists of cancellous bone at the core and cortical bone at the outer sur-

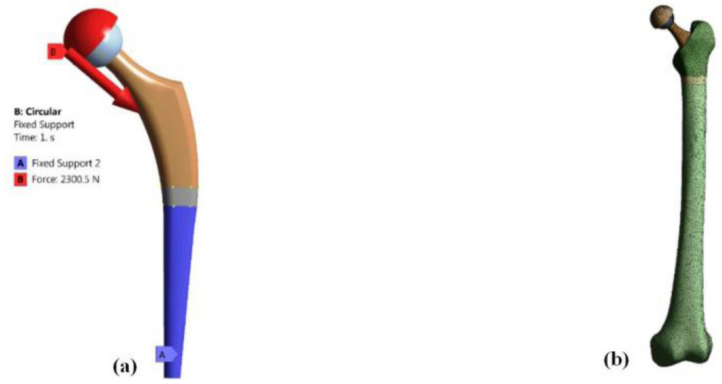

Figure 2: (a) Boundary conditions applied to the implant (b) Discretized model of the complete implant with the femur.

Table 2: Number of elements and nodes for different stem designs.

Sl	Implant designs	Total number of elements	Total number of nodes
1.	Circular	170,970	378,157
2.	Oval	163,945	341,406
3.	Ellipse	154,863	328,233
4.	Trapezoidal	160,289	334,911

face. Bone is modeled using mimics. In the implants, the stem, femoral head ball, and the backing cup are considered as CoCr material, and acetabular cups are considered as UHMWPE material.

This combination mimics the same as ceramic on polyethylene (CoPE) which are used as hip implants in the total hip arthroplasty. The static structural analysis is carried out using ANSYS R-19 to know the stresses induced in the implant along with femur and the total deformation, deformation in Z-axis, and related elastic strain. Figure 3 shows the total de-

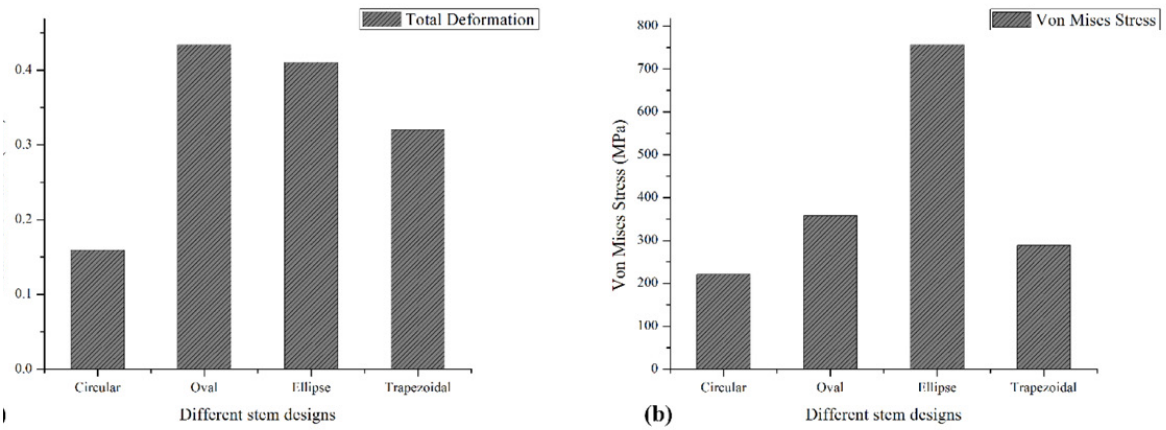

Figure 3: (a) Total deformation in mm; (b) von Mises Stress in MPa.

formation and von Mises stress of all the four designs.

The circular-shaped implant exhibited minimal total deformation of 0.16mm, comparatively lesser than the other three designs. The circular shape also showed the von Mises stresses of 218.78MPa which is lesser over the other three stem designs. Figure 4 shows the total deformation and von Mises stresses on the circular shaped hip implant along with femur.

Also, the deformation in Z-axis, due to the load applied on the backing cup, mimics the normal load transmission from the backing cup to the femur bone. Figure 5 shows the deformation in Z-axis and equivalent strain acting on the implant and femur. Circular shaped stem implant has the z-axis deformation of 0.053mm and equivalent strain of 0.003mm/mm.

Figure 6 shows the deformation in Z-axis of different stem shaped implant and also the elastic strain.

Discussion

Previously, many studies were carried out to know the behavior of different hip implant designs when subjected to static and dynamic loading conditions, but in all these studies, different boundary conditions were considered to apply load. In some studies, the distal condyle is fixed, and load is applied over the implant; in some other studies, along with distal condyle, some proportions of grater trochanter are fixed. However, in all these studies, the implants were considered safe if von Mises stresses were lesser than its yielded strength. In the present study, different stem shapes were taken into account with varying curvature and identical femoral head of 28mm, an acetabular cup of 4mm thickness, and a backing cup of 2mm thickness was modeled [36-38]. All these are fixed into the femur as for each surgical procedure. The boundary conditions are considered as per ASTM F299-13, and loading conditions are considered as per the ISO 7206-4:2010(E) [29]. Among the four designs, the circular-shaped stem shows lesser stress compared to the other three shapes. These values are identical to previous studies [15]. The circular-shaped implant has the stress values 218.78MPa and deformation of 0.16mm. The

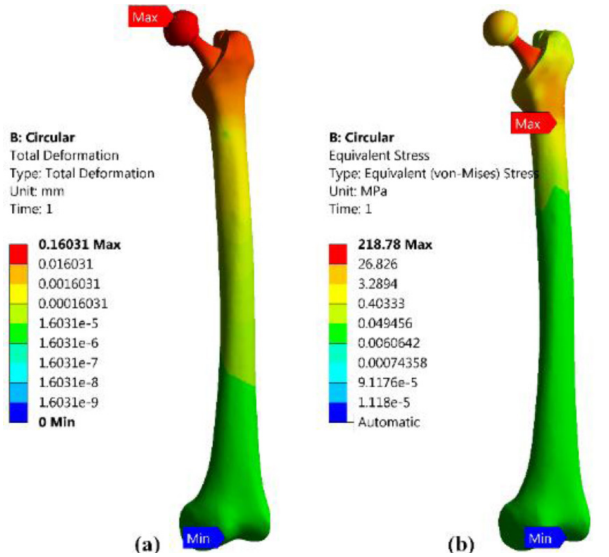

Figure 4: Circular shaped stem implant (a). Total deformation, (b). Equivalent stress (von Mises).

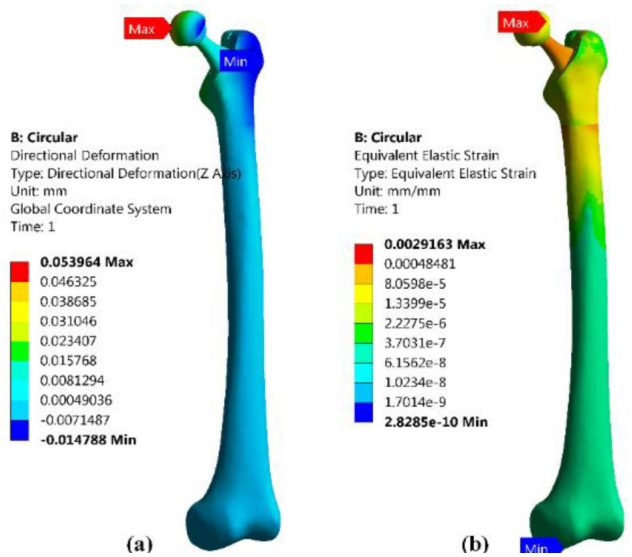

Figure 5: Circular shaped stem implant (a). Directional deformation in Z-axis, (b) Elastic strain.

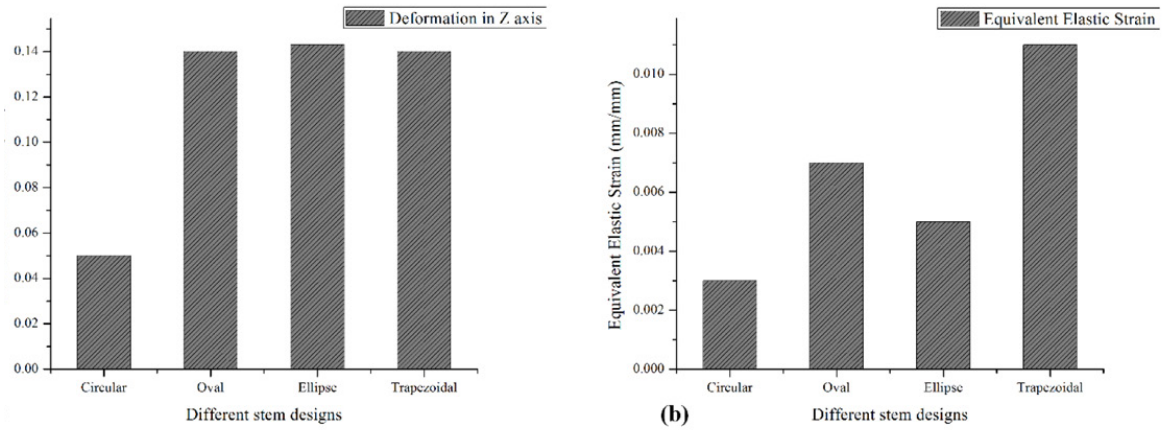

Figure 6: (a) Deformation in Z-axis in mm (b) Equivalent elastic strain in mm/mm.

stress pattern was observed almost the same in all the four designs considered for the study. The maximum total deformation was found to be at the top of the femoral head, and von Mises stresses were more at the junction where the stem is bisected from the center of the femoral head. The trapezoidal-shaped stem and circular shaped stem show the lesser stress values compared to the other two. With respect to deformation in the loading acting axis ellipse, oval and trapezoidal has shown more values which is relatively higher than the deformation in the circular-shaped designs. In this study, it is found that the cross-section shape of the stem affects the overall performance of the implant after the arthroplasty even though all other parameters are kept considered the same. Overall, the circular cross-sectioned shaped stem implant along with femur bone has least von Mises stress and deformation, which is expected to have a longer life compared to the other three designs.

Conclusion

In the current study, four hip implant designs namely circular, oval, ellipse and trapezoidal were modeled. For all the designs, the constant femoral head size of 28mm diameter, an acetabular cup of 4mm thickness and a metal backing cup of 2mm thickness were used. All these components were fixed to the stems, which were developed with the change in the cross-section. A healthy femur bone was modeled through patient-specific bone CT scans using Mimics. The femoral head was removed and implants were implanted into the femur. ASTM F2996-13 standards were considered as boundary conditions. Loading was applied as per the ISO 7206-4:2010(E), and static structural analysis was performed using ANSYS R-19. Moreover, ceramic on polyethylene was considered as implant materials. All in all, it was found that all four designs exhibited lesser stress values than the yielded strength. However, in these four designs, the circular-shaped implant had less deformation and von Mises stress. Concludingly, these designs could be used for fatigue tests under dynamic conditions to predict the life of the implant.

Acknowledgment

The authors would thank the Department of Aeronautical and Automobile Engineering, Manipal Institute of Technology, Manipal Academy of Higher Education, Manipal for

providing the high computational facility for their support in carrying out this work.

Conflict of Interest

None

References

1. Clarke B. Normal bone anatomy and physiology. Clin *J Am Soc Nephrol*. 2008;**3**:S131-9. doi: 10.2215/CJN.04151206. PubMed PMID: 18988698; PubMed Central PMCID: PMCPMC3152283.
2. Dalstra M, Huiskes R. Load transfer across the pelvic bone. *J Biomech*. 1995;**28**:715-24. doi: 10.1016/0021-9290(94)00125-n. PubMed PMID: 7601870.
3. Pan N. Length of Long Bones and their Proportion to Body Height in Hindus. *J Anat*. 1924;**58**:374-8. PubMed PMID: 17104032; PubMed Central PMCID: PMCPMC1249729.
4. Palastanga N, Field D, Soames R. Anatomy and human movement: structure and function. New York: Elsevier Health Sciences; 2012.
5. Chethan K, Shenoy BS, Bhat NS. Role of different orthopedic biomaterials on wear of hip joint prosthesis: a review. *Materials Today: Proceedings.* 2018;**5**:20827-36. doi: 10.1016/j.matpr.2018.06.468.
6. Chethan K, Bhat NS, Shenoy BS. Biomechanics of hip joint: A systematic review. International *Journal of Engineering and Technology (UAE)*. 2018;**7**:1672-6.
7. Dattani R. Femoral osteolysis following total hip replacement. *Postgrad Med J.* 2007;**83**:312-6. doi: 10.1136/pgmj.2006.053215. PubMed PMID: 17488859; PubMed Central PMCID: PMCPMC2600070.
8. Dowson D. New joints for the Millennium: wear control in total replacement hip joints. *Proc Inst Mech Eng H.* 2001;**215**:335-58. doi: 10.1243/0954411011535939. PubMed PMID: 11521758.
9. Ulrich SD, Seyler TM, Bennett D, Delanois RE, Saleh KJ, Thongtrangan I, et al. Total hip arthroplasties: what are the reasons for revision? *Int Orthop*. 2008;**32**:597-604. doi: 10.1007/s00264-007-0364-3. PubMed PMID: 17443324; PubMed Central PMCID: PMCPMC2551710.
10. Furnes O, Lie SA, Espehaug B, Vollset SE, Engesaeter LB, Havelin LI. Hip disease and the prognosis of total hip replacements. A review of 53,698 primary total hip replacements reported to the Norwegian Arthroplasty Register 1987-99. *J Bone Joint Surg Br.* 2001;**83**:579-86. doi: 10.1302/0301-620X.83B4.11223. PubMed PMID: 11380136.
11. Evans JT, Evans JP, Walker RW, Blom AW, Whitehouse MR, Sayers A. How long does a hip replacement last? A systematic review and meta-analysis of case series and national registry reports with more than 15 years of follow-up. *Lancet.* 2019;**393**(10172):647-654. doi: 10.1016/S0140-6736(18)31665-9. PubMed PMID: 30782340; PubMed Central PMCID: PMC6376618.
12. Green TR, Fisher J, Stone M, Wroblewski BM, Ingham E. Polyethylene particles of a 'critical size' are necessary for the induction of cytokines by macrophages in vitro. *Biomaterials*. 1998;**19**:2297-302. doi: 10.1016/s0142-9612(98)00140-9. PubMed PMID: 9884043.
13. Sabatini AL, Goswami T. Hip implants VII: Finite element analysis and optimization of cross-sections. *Materials & Design.* 2008;**29**:1438-46. doi: 10.1016/j.matdes.2007.09.002.
14. HQIP. National Joint Registry: 12th Annual Report 2014 Dec. Wales, Northern Ireland and the Isle of Man; 2015.
15. Colic K, Sedmak A, Grbovic A, Tatic U, Sedmak S, Djordjevic B. Finite element modeling of hip implant static loading. *Procedia Engineering*. 2016;**149**:257-62. doi: 10.1016/j.proeng.2016.06.664.
16. Chalernpon K, Aroonjarattham P, Aroonjarattham K. Static and dynamic load on hip contact of hip prosthesis and Thai femoral bones. *International Journal of Medical, Health, Biomedical, Bioengineering and Pharmaceutical Engineering*. 2015;**9**:251-5.
17. Vulovic A, Filipovic N, editors. Finite Element Analysis of Femoral Implant Under Static Load. 23-25 Oct. 2017. Washington: 17th International Conference on Bioinformatics and Bioengineering (BIBE); 2017.
18. Colic K, Sedmak A. The current approach to research and design of the artificial hip prosthesis: a review. *Rheumatol Orthop Med*. 2016;**1**:1-7. doi: 10.15761/ROM.1000106.
19. Wang M, Wang M, editors. The finite element analysis of the shape of the femoral head pros-

thesis on the influence of the hip joint. 19-21 Nov. 2017. Ningbo: IEEE International Conference on Cybernetics and Intelligent Systems (CIS) and IEEE Conference on Robotics, Automation and Mechatronics (RAM); 2017.

20. Shen FW, Lu Z, McKellop HA. Wear versus thickness and other features of 5-Mrad crosslinked UHMWPE acetabular liners. *Clin Orthop Relat Res*. 2011;**469**:395-404. doi: 10.1007/s11999-010-1555-6. PubMed PMID: 20848244; PubMed Central PMCID: PMCPMC3018202.
21. Keni LG, Kalburgi S, Hameed BZ, Zuber M, Tamagawa M, Shenoy BS. Finite Element Analysis of Urinary Bladder Wall Thickness at Different Pressure Condition. *J Mech Med Biol.* 2019:1950029. doi: 10.1142/S0219519419500295.
22. Chethan K, Zuber M, Bhat SN, Shenoy SB. Comparative study of femur bone having different boundary conditions and bone structure using finite element method. *Open Biomed Eng J.* 2018;**12**:115-34. doi: 10.2174/1874120701812010115.
23. Cerveri P, Manzotti A, Baroni G. Patient-specific acetabular shape modelling: comparison among sphere, ellipsoid and conchoid parameterisations. *Comput Methods Biomech Biomed Engin.* 2014;**17**:560-7. doi: 10.1080/10255842.2012.702765. PubMed PMID: 22789071.
24. Radcliffe IA, Prescott P, Man HS, Taylor M. Determination of suitable sample sizes for multi-patient based finite element studies. *Med Eng Phys.* 2007;**29**:1065-72. doi: 10.1016/j.medengphy.2006.11.007. PubMed PMID: 17218146.
25. Dopico-Gonzalez C, New AM, Browne M. Probabilistic finite element analysis of the uncemented hip replacement-effect of femur characteristics and implant design geometry. *J Biomech.* 2010;**43**:512-20. doi: 10.1016/j.jbiomech.2009.09.039. PubMed PMID: 19896129.
26. Lee JM, Kim TS, Kim TH. Treatment of Periprosthetic Femoral Fractures Following Hip Arthroplasty. *Hip Pelvis*. 2018;**30**:78-85. doi: 10.5371/hp.2018.30.2.78. PubMed PMID: 29896456; PubMed Central PMCID: PMCPMC5990531.
27. K NC, Zuber M, Bhat NS, Shenoy BS, C RK. Static structural analysis of different stem designs used in total hip arthroplasty using finite element method. *Heliyon*. 2019;**5**:e01767. doi: 10.1016/j.heliyon.2019.e01767. PubMed PMID: 31245635; PubMed Central PMCID: PMCPMC6581841.
28. Bhaskar D, Rajpura A, Board T. Current Concepts in Acetabular Positioning in Total Hip Arthroplasty. *Indian J Orthop.* 2017;**51**:386-96. doi: 10.4103/ortho.IJOrtho_144_17. PubMed PMID: 28790467; PubMed Central PMCID: PMCPMC5525519.
29. ASTM. Standard practice for finite element analysis (FEA) of non-modular metallic orthopaedic hip femoral stems. Philadelphia: ASTM International; 2013.
30. Reimeringer M, Nuno N, Desmarais-Trepanier C, Lavigne M, Vendittoli PA. The influence of uncemented femoral stem length and design on its primary stability: a finite element analysis. *Comput Methods Biomech Biomed Engin*. 2013;**16**:1221-31. doi: 10.1080/10255842.2012.662677. PubMed PMID: 22452543.
31. Gross S, Abel EW. A finite element analysis of hollow stemmed hip prostheses as a means of reducing stress shielding of the femur. *J Biomech*. 2001;**34**:995-1003. doi: 10.1016/s0021-9290(01)00072-0. PubMed PMID: 11448691.
32. Sabatini AL, Goswami T. Hip implants VII: Finite element analysis and optimization of cross-sections. *Mater Des.* 2008;**29**:1438-46. doi: 10.1016/j.matdes.2007.09.002.
33. Darwish S, Al-Samhan A. Optimization of artificial hip joint parameters. *Materialwissenschaft und Werkstofftechnik*. 2009;**40**:218-23. doi: 10.1002/mawe.200900430.
34. Kurtz S. The Required Mechanical Properties of Hip and Knee Components. *Dexel University and Exponent*. 2003:52-7.
35. Chethan K, Bhat SN, Zuber M, Shenoy SB. Patient-specific static structural analysis of femur bone of different lengths. *Open Biomed Eng J*. 2018;**12**:108-14. doi: 10.2174/1874120701812010108.
36. Pritchett J. Very Large Diameter Polymer Acetabular Liners Show Promising Wear Simulator Results. *J Long Term Eff Med Implants.* 2016;**26**:311-9. doi: 10.1615/JLongTermEffMedImplants.2017019182. PubMed PMID:

29199616.

37. Callaghan JJ, Hennessy DW, Liu SS, Goetz KE, Heiner AD. Cementing acetabular liners into secure cementless shells for polyethylene wear provides durable mid-term fixation. *Clin Orthop Relat Res.* 2012;**470**:3142-7. doi: 10.1007/s11999-012-2380-x. PubMed PMID: 22585349; PubMed Central PMCID: PMCPMC3462859.

38. Johnson AJ, Loving L, Herrera L, Delanois RE, Wang A, Mont MA. Short-term wear evaluation of thin acetabular liners on 36-mm femoral heads. *Clin Orthop Relat Res.* 2014;**472**:624-9. doi: 10.1007/s11999-013-3153-x. PubMed PMID: 23861047; PubMed Central PMCID: PMCPMC3890177.